2005 American Control Conference
June 8-10, 2005. Portland, OR, USA

Quasipassivity-based Robust Nonlinear Control Synthesis for Flap Positioning Using Shape Memory Alloy Micro-Actuators

N. Léchevin and C.A. Rabbath

Abstract— **This paper proposes a quasipassivity-based robust nonlinear control law for the position control of a rotary flap aimed at stabilizing the free-to-roll motion of an aerial vehicle. An antagonist-type shape memory alloy micro-actuator (SMA) is used. The plant is modeled as a cascade decomposition comprising a 2nd-order, parametric-uncertain system excited by a bounded exogenous aerodynamic moment and a 1st-order heat conduction system characterized by a hysteretic output. The control objective is to warrant accurate and fast rotation of the flap at an angle determined by the outer-loop controller. The control law is obtained from subsystem decomposition that is suitable for quasipassivation by application of feedback and feedforward control. The cascade control structure is composed of 1) sliding mode control with boundary layer, which robustifies the flap positioning, and 2) PD control that compensates for the delay induced by the hysteretic characteristics of the SMA. The control scheme provides ultimate boundedness (UB) of tracking error trajectories and robustness to uncertain, bounded, stiffness constant and aerodynamic moment. Simulations validate the proposed approach.**

I. Introduction

As with the performance increase in sensors employing MEMS, it is expected that similar gains in flight control will be made with actuators based on smart structures. Owing to their sufficiently large deformation and relatively good position recovery properties, SMA is considered to be a good candidate among smart materials for small-scale flight control surface actuation. Flap actuation is performed by means of a pulley (Fig. 1). To warrant fast response times and to generate a torque that can counteract the aerodynamic moment in both directions, an antagonist SMA actuator is used [1], [2]. The two SMA wires complement each other. One wire is heated while the other is cooled. An output feedback control based on the rotation angle and the rate of the pulley provides a current command that controls the heating of the wire.

Controlling the hysteretic behavior of a SMA remains a challenging task. Model-based synthesis of controllers usually relies on the Preisach (Pr.) model and the likes [3]. [4] developed a hysteresis compensation-based adaptive control. They use the Krasnoselskii and Prokrovskii 's model (KP model) [4]. It results in good tracking properties for slowly time varying reference trajectories. Adaptive hysteresis inverse in cascade with a linear and/or nonlinear plant was proposed in the context of adaptive control [5]. To improve tracking performance, [6] proposed to augment the PID controller with a static inverse model of the 2^{nd}-order bias-type actuator in series with a modified (stochastic) Pr. model. The tracking error is free of limit cycles and works well with signals within $[0, 0.1]$ Hz. [2] proposes passivity-based stability synthesis of SMA actuation modeled as a 1^{st}-order heat transfer system in series with a Pr. model. This approach results in PID controllers achieving L_2-stability of the closed-loop system from the command to the position or speed tracking error [2]. Only a static load is considered and an extension to the dynamic case is necessary for the flap positioning. Other approaches use varying time delay modelling of the hysteresis. Time-delay control is applied to stabilize a bias-type SMA [7]. An interesting approach consists in interpreting the hysteresis as a phase lag in the frequency domain and to compensate for it within a given bandwidth by means of a phase lead compensator [8]. Variable structure controller (VSC) has been proposed to stabilize an antagonistic-type SMA actuator [1]. The controller provides robustness, small limit cycles and is easy to implement.

This paper proposes a robust nonlinear control law for the position control of a rotary flap. An antagonist-type SMA micro-actuator achieves the rotation. Trajectory tracking requires 1) warranting robustness to uncertainties (unknown aerodynamic moment, stiffness and viscous friction) and 2) achieving satisfactory closed-loop performances despite the hysteresis. The rationale of the design is: employ VSC to obtain robust performance, phase-lead compensator to quasipassivate the SMA dynamics and quasipassivity-based analysis that warrants robust UB of system trajectories. A two-step procedure is carried out: (i) assuming that the actuator is ideal, a VSC law is designed to robustly stabilize the flap dynamics and to quasi-passivate an appropriate I/O signal pair of the forward path; (ii) a phase-lead, open-loop compensator is synthesized to render the feedback path (SMA micro-actuator), strictly input quasi-passive [9]. The control synthesis relies on the KP model of the hysteresis [4]. The feedback connection of the two paths leads to UB of tracking error trajectories of the plant despite uncertainties in the dynamic loads and in the friction.

N. Lechevin is with Defence Research and Development Canada - Valcartier, 2459 Pie-XI N., Val-Belair, Qc, Canada G3J 1X5 and Université du Québec à Trois-Rivières, Trois-Rivières, Qc, Canada G9A 5H7

C.A. Rabbath is with Defence Research and Development Canada - Valcartier and Department of Mechanical Engineering, McGill University, Montreal, Qc, Canada H3A 2K6

This work was partly funded through DRDC TIF project entitled 'Supersonic Missile Flight Control by Manipulation of the Flow Structure using Microactuated Surfaces'.

II. Actuator Modeling

A. Structure

In Fig. 1, one SMA fiber in phase transition is generating a contraction force while the other is expanding. The objective of the control law is to rotate the flap to track a time-varying trajectory. The trajectory is provided by an outer-loop control law.

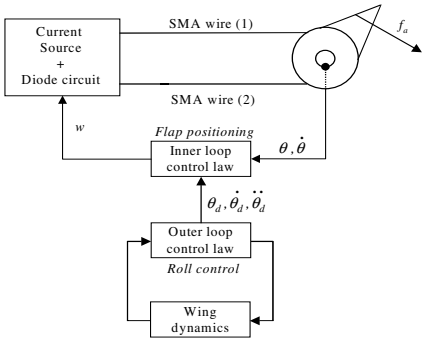

Figure 1: Structure of actuator with control law

The pulley has diameter $2r$ and rotation angle θ, which induces the linear displacement x of the wires. The dynamics under study is depicted in Fig. 2 where the switching nature of the actuator is shown. The control law has for input the rotation angle and the rate of the pulley. The controller output is a current command that controls the wire heating by means of a diode-based circuit. To obtain the model of the actuator, assume that SMA fibers satisfy the following assumption.

Assumption 1 At any given time, SMA1 in Fig.2 is heated. SMA1 is then generating a force that can be decomposed into the following components:

1) The stiffness of SMA1

$$\delta f_{1s} = k_{s1} r \delta\theta = k_{s1} \delta x \tag{1}$$

where δf_{1s} , k_{s1}, $\delta\theta$ and δx respectively represent the change in the opposing force, the stiffness constant, the change in the angle of rotation and the linear displacement of the fiber extremity.

2) The contraction force, $\delta f c_1 = k_{c1} h_1(\widetilde{T})$, generated by the transition between the martensitic phase and the austenitic phases [6], [7] where $\widetilde{T}$ is the difference between wire temperature and ambient temperature, and $h_1(\widetilde{T})$ describes the hysteresis of the SMA as a nonlinear function of $\widetilde{T}$. Constants k_{s1} and k_{c1} depend on the physical parameters of the SMA [6], [7]. Since it is in the cool phase, fiber SMA2 shown in Fig. 2 is malleable and thus its deformation requires a force f_{d2} whose magnitude is bounded above by F_d and is significantly smaller than $f c_1$. ⋈

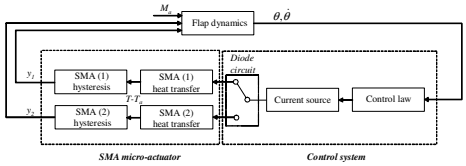

Figure 2: Block diagram of SMA and control system

Applying Newton's law and from Assumption 1, the motion of the actuator can be described as

$$J\ddot{\theta} + \rho\dot{\theta} + k_{si} r^2 \theta = -k_{ci} r h_i(\widetilde{T}) - r f_{dj} - M_a \tag{2}$$

where J is the moment of inertia of the pulley and the flap, $\rho < \rho_M$ is a damping coefficient and M_a is the aerodynamic moment applied on the flap and is assumed to be bounded $|M_a| \leq \Gamma$. Index $i = 1, 2$ denotes the wire under heating and $j = 1, 2$ the remaining wire that acts in a complementary fashion, i.e. the wire under cooling. The geometry of the fiber is such that the 1D heat conduction problem of the SMA can be approximated by the 1^{st}-order dynamics

$$\begin{cases} d\widetilde{T}/dt = -a\widetilde{T} + bu \\ y_i = h_i(\widetilde{T}) \end{cases} \tag{3}$$

where the control variable u, y_i, a and b respectively represent the electric power delivered by a power amplifier, the hysteresis of the SMA and the heating parameters. As noticed in (2), the term $h_i(T)$ ensures the connection between the heating dynamics and the flap dynamics.

B. Krasnoselskii and Prokrovskii's model

The Pr. model is commonly used for control design [2], [3]. However, we propose to employ a numerical version of the Krasnoselskii and Prokrovskii's (KP) model [4] which is best suited to the quasipassivity approach for controller synthesis. Suppose the Pr. triangle over which the hysteresis occurs, which is defined as

$$S = \{s \in R : s = (s_1, s_2), s_1 \geq s_2\}, \tag{4}$$

is divided into a mesh grid of K horizontal lines and K vertical lines. With $\widetilde{T}_{\min}$ and $\widetilde{T}_{\max}$ defined as relative temperature bounds, the KP model can be expressed as [4]

$$h(T) = \sum_{i=1}^{K} \sum_{j=1}^{K} \left[k_{s_{ij}}(\widetilde{T}, \xi_{ij}) \right](t) \theta_{ij} + m\widetilde{T}. \tag{5}$$

In (5), $0 < m \ll 1$, θ_{ij} are weighting values for the $s_{ij} = (s_i, s_j)$ pairs, ξ_{ij} is a memory term updated whenever $d\widetilde{T}/dt$ changes sign, and [4]

$$k_{s_{ij}} = \begin{cases} \max(\xi_{ij}, r(\widetilde{T} - s_j)), & \text{for } d\widetilde{T}/dt \geq 0 \\ \min(\xi_{ij}, r(\widetilde{T} - s_i)), & \text{for } d\widetilde{T}/dt \leq 0 \end{cases} \quad (6)$$

where the relay with finite slope ridge functions $r(\widetilde{T})$ is given as [4]

$$r(x) = \begin{cases} -1, & x < 0 \\ \frac{2x}{a} - 1, & 0 \leq x \leq a \\ 1, & x > a \end{cases} \quad (7)$$

where $a = (\widetilde{T}_{\max} - \widetilde{T}_{\min})/(K-1)$. The θ_{ij} are assumed to be bounded, piecewise continuous and nonnegative inside S [2]. The numerical version of the KP model (5) along with its kernel function (6)-(7) enable formulating the hysteresis as a piecewise affine function of the temperature variation

$$h(\widetilde{T}) = k(\widetilde{T})\widetilde{T} + \xi(\widetilde{T}) \quad (8)$$

with

$$k(\widetilde{T}) = m + \begin{cases} k_1, & \text{if } \widetilde{T} \in \left[\widetilde{T}_{\min}, \widetilde{T}_{\min} + a\right) \\ k_2, & \text{if } \widetilde{T} \in \left[\widetilde{T}_{\min} + a, \widetilde{T}_{\min} + 2a\right) \\ \vdots & \vdots \\ k_K, & \text{if } \widetilde{T} \in \left[\widetilde{T}_{\max} - a, \widetilde{T}_{\max}\right) \end{cases} \quad (9)$$

and $k_i > 0$, $i = 1, ..., K$, are piecewise temperature-varying linear combinations of the slope $(2/a)$ of the elementary relays. The term $\xi(\widetilde{T})$ in (8) is the total memory of the alloy and is obtained by a linear combination of the residual memory of the relays. Since parameters (8) result from finite linear combinations, the following bounds can be established

$$\begin{aligned} 0 < K_m \leq k(\widetilde{T}) \leq K_M \\ \xi_m \leq \xi \leq \xi_M. \end{aligned} \quad (10)$$

III. Quasipassivity-based Stabilization

To warrant robust UB of the nonlinear system given by (2), (3), (8), (10) around the desired trajectory given as $\left(\theta_d, d\theta_d/dt, \widetilde{T}_d\right)$, a quasipassivity-based control synthesis is carried out as follows. First, a suitable feedback decomposition of (2)-(3) with connection relation (8) is proposed. Second, each subsystem is made strictly quasipassive by means of the control law. The composition of each local controller constitutes the control law of the SMA-actuated flap. Then, from classical arguments of quasipassivity, UB of system trajectories follow [9]. The definition of strict quasipassivity and quasipassivity [9] are given as follows.

Definition 1 Consider a nonlinear system given as $\dot{x} = f(x, v, u)$, $z = h(x, v, u)$ where x is the state, v is an exogenous input used to define the supply rate, u is the control input and y represents the output.

1) If there exists a control input signal u such that $z^T v \geqslant \gamma(\|x\|) + \dot{V}(x)$ is satisfied with $\gamma(\|x\|) > 0$ when $0 < D \leq \|x\|$ and V is positive definite, then the input-output pair (v, z) is *strictly quasipassive*. If $D = 0$, (v, y) is a passive pair.

2) If there exists $\chi > 0$ and a control input signal u such that $z^T v + \chi \geqslant \dot{V}(x)$ is satisfied then the input-output pair (v, z) is *quasipassive*. If $\chi = 0$, (v, y) is a passive pair. $\bowtie$

For the derivation of the variable structure controller, the following assumption on the desired trajectories and the physical limits of the actuator is assumed to hold.

Assumption 2 The desired trajectory obtained by means of the outer-loop controller of Fig. 1 is smooth enough to consider the following bounds

$$\begin{aligned} |\theta_d| &\leq M_1 \\ |\dot{\theta}_d| &\leq M_2 \\ |\ddot{\theta}_d| &\leq M_3 \end{aligned} \quad (11)$$

where $M_k \in \mathcal{R}$, $k = 1, 2, 3$. Furthermore, the physical limits of the actuator impose bounds on the angle and speed of rotation as

$$\begin{aligned} |\theta| &\leq N_1 \\ |\dot{\theta}| &\leq N_2 \end{aligned} \quad (12)$$

where $N_k \in \mathcal{R}$, $k = 1, 2$.

A. Quasipassive Subsystem Decomposition

Consider Fig. 3, where the block labeled flap dynamics corresponds to (3), the block denoted as SMA micro-actuator corresponds to (2), and w is the actual control input. The control law to be synthesized is divided into subsystems C_1 and C_2 expressed as

$$(C_1) \quad : \quad \left(\theta, \dot{\theta}, \theta_d, \dot{\theta}_d, \ddot{\theta}_d\right) \mapsto u \quad (13)$$

$$(C_2) \quad : \quad w = k_p u + k_d \dot{u} \quad (14)$$

where k_p, $k_d \in \mathcal{R}^+$ are the control gains.

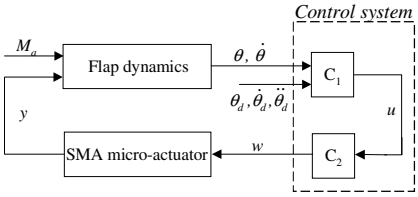

Figure 3: Feedback decomposition

A passive decomposition of the system shown in Fig. 3 can be obtained by adding and subtracting signal u, as shown in Fig. 4.

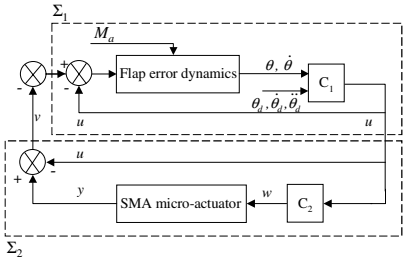

Figure 4: Passive feedback decomposition

Taking u as the output of Σ_1 and substituting for the dynamics in (2) and the passivating law C_1 in (13) to be designed, one obtains the closed-loop system Σ_1

$$\Sigma_1 : \begin{cases} \frac{d}{dt}\begin{bmatrix} \widetilde{x}_1 \\ \widetilde{z} \end{bmatrix} = \\ f\left(\widetilde{x}_1, z, \dot{\theta}_d, \ddot{\theta}_d, \dddot{\theta}_d, f_{d_2}, M_a\right) - \begin{bmatrix} 0 \\ 1 \end{bmatrix} b_1 v \\ u = C_1\left(\widetilde{x}_1, z, \theta_d, \dot{\theta}_d, \ddot{\theta}_d\right). \end{cases} \tag{15}$$

where $b_1 = k_{ci} r/J$, $v = y_i - u$ and $f : \mathcal{R}^{7\times 1} \rightarrow \mathcal{R}$. State variables $\widetilde{x}_1$ and z as well as function f are defined in the next section. Similarly, using (3) and the structure of Fig. 3, the following expression for Σ_2 can be obtained:

$$\Sigma_2 : \begin{cases} \dot{\widetilde{\varsigma}} = -a\varsigma + u \\ \widetilde{T} = c\varsigma + b_2 k_d u \\ v = y - u = k(\widetilde{T})\widetilde{T} + \xi(\widetilde{T}) - u \end{cases} \tag{16}$$

where $c = b_2\left(k_p - a k_d\right)$ and $\varsigma = b_2\left(k_p \widetilde{T} + k_d d\widetilde{T}/dt\right)$.

The control law corresponding to C_1 and C_2 has to render Σ_1 strictly quasipassive and Σ_2 quasipassive to warrant closed-loop stability. With the objective of obtaining a robust closed-loop system, robust strict quasipassivity is required for Σ_1 since the aerodynamic moment and the friction are uncertain. Hence, UB of Σ_1 in closed-loop with Σ_2 is obtained by direct application of the quasipassive equivalent of the passivity theorem [9]. On the one hand, Σ_1 is the stabilized flap positioning system in closed-loop with the state-feedback control law C_1. On the other hand, Σ_2 represents the micro-actuator dynamics in open-loop with the feedforward controller C_2, which quasipassivates Σ_2 for the pair (u, v). By applying quasipassivity results for interconnected systems, it follows that strict quasipassivation of both Σ_1 and Σ_2 can be achieved in the sense that Σ_1 is made robust to the quasipassive and stabilized uncertain system Σ_2.

B. Control law synthesis

This section describes the synthesis of C_1 and C_2 shown in Fig. 3 and 4.

1) Synthesis of C_1: In this section, the tracking error dynamics of Σ_1 (2) is used. Explicit systems (2) as

$$\begin{cases} \dot{\widetilde{x}}_1 = -\lambda \widetilde{x}_1 + z \\ \dot{z} = \delta - b_1(u + v) \end{cases} \tag{17}$$

with

$$\begin{gathered} \widetilde{x}_1 = x_1 - x_1^d \\ \widetilde{x}_2 = x_2 - x_2^d \\ z = x_2 + \lambda \widetilde{x}_1 - x_2^d \\ v = y_i - u \\ \delta = (\lambda - \alpha) x_2 - \beta x_1 + \lambda x_2^d - \dot{x}_2^d - \eta f_{dj} - M_a \end{gathered} \tag{18}$$

and where $x_1 = \theta$, $x_2 = \dot{x}_1$, $x_1^d = \theta_d$, $x_2^d = \dot{x}_1^d$, $\alpha = \rho/J < \alpha_M$, $\beta = k_{si} r^2/J$, $\eta = r/J$ and $\lambda > 0$ is a tuning parameter. The control input u must be such that system Σ_1, given by (17) in closed-loop with C_1, is quasipassive for the input-output pair $(-v, u)$.

Proposition 1 The variable structure control law given by

$$u = (\mathcal{U}/b_1)\tanh\left(\frac{z}{\varepsilon}\right),\ \varepsilon > 0 \tag{19}$$

results in Σ_1 being strictly quasipassive for the pair $(-v, u)$ provided

$$\begin{gathered} \mathcal{U} = 2(\Delta + \mu) \\ \mu > \varepsilon b_1^2 (M_1 + N_1) \end{gathered} \tag{20}$$

where $\Delta > |\delta| <$ and $\mu > \varepsilon b_1^2 (M_1 + N_1)$. $\bowtie$

Remarks 1) From Assumption 2, the bound Δ on δ is computed as

$$|\delta| < (\lambda + \alpha_M) N_2 + \beta N_1 + \lambda M_2 + M_3 + \eta F_d + \Gamma = \Delta. \tag{21}$$

2) As usually done in the synthesis of variable structure control, the choice of constant $\varepsilon > 0$ results from a trade-off between an acceptable boundary layer in terms of steady-state error and minimization of chattering. 3) Constant μ in (20) is chosen such that it bounds the nonsingular term $b_1^2 \widetilde{x}_1 z/\tanh\left(\frac{z}{\varepsilon}\right)$, which will appear in the forthcoming Lyapunov-based stability analysis, given that

$$\left| b_1^2 \widetilde{x}_1 z/\tanh\left(\frac{z}{\varepsilon}\right)\right| < \varepsilon b_1^2 \widetilde{x}_1. \tag{22}$$

Proof of Proposition 1: The time-derivative of the following positive definite storage function

$$V(\widetilde{x}, z) = \mathcal{U}/2\widetilde{x}_1^2 + (\epsilon \mathcal{U}/b_1^2)\ln\left|\cosh\left(\frac{z}{\epsilon}\right)\right|, \tag{23}$$

which will also serve as a Lyapunov function candidate, is expressed as

$$\begin{gathered} \dot{V}(\widetilde{x}, z) = \mathcal{U}\left(-\lambda \widetilde{x}_1^2 + \widetilde{x}_1 z\right. \\ \left. + \tanh\left(\frac{z}{\epsilon}\right)(\delta - b_1(u + v))/b_1^2\right). \end{gathered} \tag{24}$$

By definition of $\mathcal{U}$, there exists $z_\varepsilon > 0$ such that

$$\left|(\mathcal{U}/2)\tanh\left(\frac{z}{\varepsilon}\right)\right| \leq \sup\left|\delta + b_1^2 \widetilde{x}_1 z/\tanh\left(\frac{z}{\varepsilon}\right)\right| \tag{25}$$

for all $|z| \leq z_\varepsilon$,

$$(\mathcal{U}/2)\tanh\left(\frac{z}{\varepsilon}\right) > \sup\left|\delta + b_1^2 \widetilde{x}_1 z/\tanh\left(\frac{z}{\varepsilon}\right)\right| \tag{26}$$

for all $z > z_\varepsilon$ and

$$(\mathcal{U}/2)\tanh\left(\frac{z}{\varepsilon}\right) < -\sup\left|\delta + b_1^2 \widetilde{x}_1 z/\tanh\left(\frac{z}{\varepsilon}\right)\right| \tag{27}$$

for all $z < -z_\varepsilon$. Therefore,

$$\begin{gathered} \dot{V}(\widetilde{x}, z) = -\lambda \mathcal{U} \widetilde{x}_1^2 + (\mathcal{U}/b_1^2)\tanh\left(\frac{z}{\epsilon}\right) \\ \times \left(b_1^2 \widetilde{x}_1 z/\tanh\left(\frac{z}{\varepsilon}\right) + \delta - b_1(u + v)\right). \end{gathered} \tag{28}$$

Considering the definition of control input u (19) and properties (25), (26) and (27) of $\mathcal{U}$, then for all $|z| > z_\varepsilon$ the following state strict passivity inequality [10] is obtained for the pair $(-v, u)$

$$\dot{V}(\widetilde{x}, z) \leq -\lambda \mathcal{U} \widetilde{x}_1^2 - \frac{\mathcal{U}^2}{2b_1^2}\tanh^2\left(\frac{z}{\epsilon}\right) - vu. \tag{29}$$

Such inequality cannot be satisfied whenever $|z| < z_\varepsilon$ since u does not necessarily dominate terms in δ and $\widetilde{x}_1 z$. Therefore, obtaining inequality (29) leads to the conclusion that system Σ_1 is strictly quasipassive for the pair $(-v, u)$.□

2) Synthesis of C_2: Analysis of quasipassivity of Σ_2 is performed by considering the PD compensator C_2 whose implementation is described in the next section.

Proposition 2 With the selection of the positive definite storage function given by

$$W(\varsigma) = ck(\widetilde{T})\frac{\varsigma^2}{2}, \tag{30}$$

controller C_2 given by (14) results in Σ_2 being quasipassive for the pair (v, u) provided

$$\begin{array}{l} k_d > \frac{3}{2b_2 K_m} \\ k_p > a k_d. \bowtie \end{array} \tag{31}$$

Proof: Recall that $k(\widetilde{T})$ is a piecewise constant and positive function of $\widetilde{T}$, then the time-derivative of W is expressed as

$$\dot{W}(\varsigma) = ck(\widetilde{T})\left(-a\varsigma^2 + \frac{u\widetilde{T}}{c} - \frac{k_d u^2}{c'}\right). \tag{32}$$

From the definition of y (3)-(8), (32) becomes

$$\begin{array}{l} \dot{W}(\varsigma) = -ck(\widetilde{T})a\varsigma^2 - b_2 k_d k(\widetilde{T})u^2 + yu - \xi u \\ = -ck(\widetilde{T})a\varsigma^2 - \frac{1}{2}(u+\xi)^2 \\ -\left(b_2 k_d k(\widetilde{T}) - \frac{1}{2}\right)u^2 + yu + \frac{\xi^2}{2}. \end{array} \tag{33}$$

From the last equality of (16), $\dot{W}(\varsigma)$ satisfies the following inequality

$$\dot{W}(\varsigma) \le -ck(\widetilde{T})a\varsigma^2 - \left(b_2 k_d k(\widetilde{T}) - \frac{3}{2}\right)u^2 + vu + \frac{\xi_M^2}{2} \tag{34}$$

which means from Definition 1 that Σ_2 is quasipassive for pair (v, u) .□

C. Closed-loop Stability

Controllers C_1 (13) and C_2 (14) can be shown to provide closed-loop stability for the structure of Fig. 4.

Theorem 1 The control law composed of C_1 (13) in series with C_2 (14) in closed-loop with the plant (2)-(3), which is uncertain in the aerodynamic moment M_a acting on the flap and in the friction ρ, provides UB of the trajectories of the error dynamics provided conditions (20) and (31) are satisfied. The ultimate bound is defined as

$$b_{z_b} = \cosh^{-1}\left(\exp\left(\frac{L}{l}z_b^2\right)\right) \tag{35}$$

with $z > z_b$ and $z_b = \max\left(z_\varepsilon, \varepsilon\tanh^{-1}\left(\frac{b_1\xi_M}{b_2 k_d K_m \mathcal{U}}\right)\right)$. ⋈

In the proof of Theorem 1, the following lemma is used.

Lemma 1 The following inequality

$$\begin{array}{c} \ln\left|\cosh\left(\sqrt{x^2+y^2}\right)\right| \\ \le \ln|\cosh(x)| + \ln|\cosh(y)| \end{array} \tag{36}$$

holds for all $x, y \le R$. ⋈

Proof: Let $f(x) = \ln|\cosh(x)|$. f is a convex function. Assume that (36) is false, hence by a convexity argument

$$\begin{array}{l} f(\sqrt{x^2+y^2}) > f(x) + f(y) \\ > 2f\left(\frac{x+y}{2}\right) \end{array} \tag{37}$$

for which a counter-example is easily found; for instance, with $x = 3$, $y = 4$ one obtains $f(5) = 4.3$ and $2f(3.5) = 5.6$. □

Proof of Theorem 1: From the definition of v in (16), the first equation of (33) can be rewritten as

$$\begin{array}{l} \dot{W}(\varsigma) = -ck(\widetilde{T})a\varsigma^2 - \left(b_2 k_d k(\widetilde{T}) + 1\right)u^2 + vu - \xi u \\ \le -ck(\widetilde{T})a\varsigma^2 + vu. \end{array} \tag{38}$$

Inequality (38) holds true whenever $|u| > \xi_M/(b_2 k_d K_m + 1)$. Therefore, from (29) and (38), the interconnection of Σ_1 and Σ_2 leads to the following energy-like balance inequality

$$\begin{array}{l} \dot{U}(\widetilde{x}, z, \varsigma) = \dot{V}(\widetilde{x}, z) + \dot{W}(\varsigma) \\ \le -\lambda\mathcal{U}\widetilde{x}_1^2 - \frac{\mathcal{U}^2}{2b_1^2}\tanh^2\left(\frac{z}{\epsilon}\right) - ck(\widetilde{T})a\varsigma^2 \end{array} \tag{39}$$

for all $|z| > z_\varepsilon$ and $|u| > \xi_M/(b_2 k_d K_m)$; that is, for all $z > \varepsilon\tanh^{-1}(\xi_M b_1/b_2 k_d K_m \mathcal{U})$. Therefore, the positive definite function $U(\widetilde{x}, z, \varsigma)$ is decreasing along the system trajectories whenever $z > z_b$. This shows that the plant trajectories are ultimately bounded [10].

From Lemma 1 and considering the fact that the inequality $\ln|\cosh(x/\varepsilon)| \le (x/\varepsilon)^2$ holds for all $x \le R$, the storage function W is respectively lower- and upper-bounded by positive definite functions

$$\begin{array}{c} W_1(\widetilde{x}, z, \varsigma) = L\|X\|^2 \\ W_2(\widetilde{x}, z, \varsigma) = l\ln|\cosh(X)| \end{array} \tag{40}$$

with $L = \max\left(\frac{\mathcal{U}}{2}, \frac{\mathcal{U}}{\varepsilon b_1^2}, cK_M\right)$, $l = \min\left(\frac{\mathcal{U}}{2}, \frac{\mathcal{U}}{b_1^2}, cK_m\right)$ and $X = \begin{bmatrix} \widetilde{x} & z & \varsigma \end{bmatrix}^T$. Therefore, from [10], W_1 and W_2 can be used to determine the ultimate bound b_{z_b} of system trajectories as $b_{z_b} = W_1^{-1}(W_2(z_b))$, which leads to (35). □

Remarks 1) The magnitude of the ultimate bound and consequently of the flap positioning steady-state error depends on ε and on the maximum memory of the SMA ξ_M and can be reduced by decreasing ε provided chattering is avoided, and by increasing k_d and k_p accordingly. 2) The PD control law C_2 can be viewed as a phase-lead controller [8], which compensates within a given bandwidth for the delay introduced by the hysteresis. 3) Since the variable structure controller is differentiable, compensator C_1 in series with C_2 can be computed as follows

$$w = \mathcal{U}\left(k_p/2\sinh(\frac{2z}{\varepsilon}) + k_d\dot{z}\right)/\left(b_1\cosh^2\left(\frac{z}{\varepsilon}\right)\right) \tag{41}$$

where $\dot{z}$ necessitates, from (18), the computation of $d^2\theta_d/dt^2$ and the measurement, or the approximated computation, of $d^2\theta/dt^2$ by means of numerical filtered differentiation.

IV. Numerical Simulations

The control law composed of C_1 (13) in series with C_2 (14) is simulated. Each SMA wire has a total length of 23 cm, a diameter of 0.5 mm and can be deformed up to 10 mm. At $t = 0$, the system is at equilibrium and each SMA is initially deformed to 5 mm. The following parameters are used in the simulations: $r = 2$ cm, $J = 10^{-6}$kg.m^2, $\rho = 2 \cdot 10^{-3}$ kg.m^2.s^{-1}, -3 N $\leq f_a \leq 3$ N. The ambient temperature is fixed to 273 K. Controller gains are set to $\mathcal{U} = 5$, $\varepsilon = 0.05$, $K_p = 2$ and $K_d = 10^{-3}$ to provide acceptable performance within [1 Hz, 10 Hz] . A set-point regulation with $\theta_d = 14.3^o$ and the tracking stabilization of a sinusoidal signal (10 Hz) are carried out along with an unknown exogenous disturbance $M_a = rf_a$ where: (i) f_a =0 N, for $0 \leq t < 0.05$ s, (ii) $f_a = 3$ N for 0.05 s $\leq t < 0.01$ s and (iii) $f_a = -3$ N for 0.01 s $\leq t < 0.015$ s

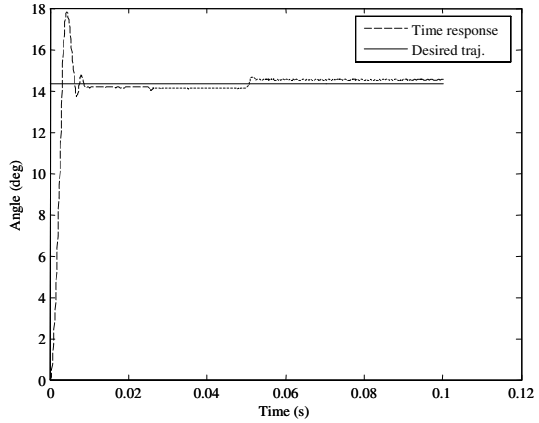

Figure 5: Set-point regulation of flap angle

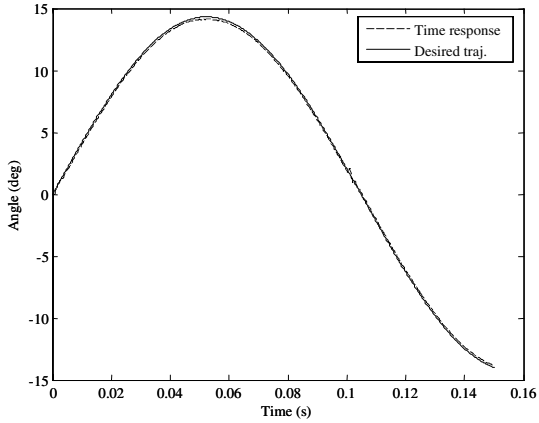

Figure 6: Sinusoidal trajectory tracking

As shown in Fig. 5, the angle trajectory has a response time smaller than 100 ms, which is fast enough to meet the requirement of the outer-loop stabilizer of Fig. 1. The boundary layer results in a small steady-state error. As anticipated, the controller exhibits robustness properties as the time-response is relatively insensitive to non-null values of M_a. Tracking of a sinusoidal trajectory leads, as shown in Fig. 6, to a steady state error less than 3% which is acceptable for flap positioning.

V. Conclusions

This paper presented a quasipassivity-based robust nonlinear control law for the position control of a rotary flap. Assuming the actuator is ideal, a VSC law is designed to robustly stabilize the flap dynamics and to quasipassivate an appropriate I/O signal pair of the forward path. Then, a phase-lead, open-loop compensator is synthesized to render the feedback path (SMA micro-actuator) strictly input quasipassive. The design relies on the KP model of the hysteresis. The trajectories of the closed-loop system are robustly ultimately bounded with respect to the aerodynamic moment and the viscous friction. Numerical simulations validated the proposed approach.

Acknowledgement

The authors would like to thank Dr. Wong for enlightening discussions on the project.

References

[1] D. Grant and V. Hayward, "Variable Structure Control of Shape Memory Alloy Actuators," *IEEE Control systems Magazine*, Vol. 17, No. 3, pp. 80-88, 1997.

[2] R.B. Gorbet, A. Morris and D.W.L. Wang, "Passivity-Based Stability and Control of Hysteresis in Smart Actuators,"*IEEE Transactions on Control Systems Technology,* Vol. 9, No. 1, pp. 5-16, January 2001.

[3] I.D. Mayergoyz, *Mathematical Models of Hysteresis*, New York: Springer-Verlag, 1991.

[4] G.V. Webb, D.C. Lagoudas and A.J. Kurdila, "Hysteresis Modeling of SMA Actuators for Control Applications," *Journal of Intelligent Material Systems and Structures,* Vol. 9, pp. 432-448, June 1998.

[5] G. Tap and P. Kokotovic, *Adaptive Control of Systems with Actuator and Sensor Nonlinearities*, New York, Wiley, 1996.

[6] S. Majima, K. Kodama and T. Hasegawa, "Modeling of Shape Memory Alloy Actuator and Tracking Control System with the Model," *IEEE Transactions on Control Systems Technology,* Vol. 9, No. 1, pp. 54-59, January 2001.

[7] H.J. Lee and J.J. Lee, "Time Delay Control of a Shape Memory Alloy Actuator,"*Journal of Intelligent Material Systems and Structures,* Vol. 13, pp. 227-239, 2004.

[8] J.M. Cruz-Hernandez and V. Hayward, "Phase Control Approach to Hysteresis Reduction," *IEEE Transactions on Control Systems Technology,* Vol. 9, No. 1, pp. 17-26, January 2001.

[9] I.G. Polushin and H.J. Marquez, "Boundedness Properties of Nonlinear Quasi-Dissipative Systems," *IEEE Transactions on Automatic Control*, vol.. 49, no.. 12, December 2004 pp.2257-2261.

[10] H.K. Khalil, *Nonlinear Systems*, 3^{rd} edition, Prentice-Hall, Upper Saddle River, NJ, 2001.